Naval Research Laboratory
Washington, DC 20375-5320

U.S. NAVAL RESEARCH LABORATORY

NRL/6930/MR—2021/2

NRL NISE - Electrochemical Detection of Heavy Metals and Polyfluoroalkyl-Compounds

SCOTT A. TRAMMELL
JEFFREY S. ERICKSON

Laboratory for Molecular Interfaces
Center for Bio/Molecular Science & Engineering

LISA C. SHRIVER-LAKE

Laboratory for Biomaterials and System
Center for Bio/Molecular Science & Engineering

SCOTT N. DEAN
DANIEL ZABETAKIS

Laboratory for Bio/Nano Science and Technology
Center for Bio/Molecular Science & Engineering

JENIFER R. HAJZUS

American Society for Engineering Education
Washington, DC

DAN J. PENNACHIO

National Research Council
Washington, DC

RACHAEL L. MYERS-WARD

Power Electronics Materials Section
Electronics Science and Technology Division

November 5, 2021

REPORT DOCUMENTATION PAGE

Form Approved
OMB No. 0704-0188

1. REPORT DATE *(DD-MM-YYYY)*	**2. REPORT TYPE**	**3. DATES COVERED** *(From - To)*
05-11-2021	NRL Memorandum Report	Oct. 1, 2020 – Sept. 30, 2021

4. TITLE AND SUBTITLE

NRL NISE - Electrochemical Detection of Heavy Metals and Polyfluoroalkyl-Compounds

5a. CONTRACT NUMBER

5b. GRANT NUMBER

5c. PROGRAM ELEMENT NUMBER

6. AUTHOR(S)

Scott A. Trammell, Jeffrey S. Erickson, Lisa C. Shriver-Lake, Scott N. Dean,
Daniel Zabetakis, Jenifer R. Hajzus*, Dan J. Pennachio**, and Rachael L. Myers-Ward

5d. PROJECT NUMBER

5e. TASK NUMBER

5f. WORK UNIT NUMBER
1X52

7. PERFORMING ORGANIZATION NAME(S) AND ADDRESS(ES)

Naval Research Laboratory
4555 Overlook Avenue, SW
Washington, DC 20375-5320

8. PERFORMING ORGANIZATION REPORT NUMBER

NRL/6930/MR--2021/2

9. SPONSORING / MONITORING AGENCY NAME(S) AND ADDRESS(ES)

Naval Research Laboratory
4555 Overlook Avenue, SW
Washington, DC 20375-5320

10. SPONSOR / MONITOR'S ACRONYM(S)

NRL

11. SPONSOR / MONITOR'S REPORT NUMBER(S)

12. DISTRIBUTION / AVAILABILITY STATEMENT

DISTRIBUTION STATEMENT A: Approved for public release; distribution is unlimited.

13. SUPPLEMENTARY NOTES

*American Society For Engineering Education, 1818 N. Street N.W., #600, Washington, DC 20036
**National Research Council, 500 Fifth Street NW, Washington, DC 20001

14. ABSTRACT

The electrochemical detection of heavy metals and polyfluoroalkyl-compounds are reported using an inexpensive in-house built potentiostat, the CStat. For heavy metal detection, two types of epitaxial graphene were used as a working electrode; multilayer graphene and hydrogen-intercalated, quasi-freestanding bilayer graphene. In addition, the graphene types were modified with an O2 plasma etch to introduce oxygen chemical groups to the surface of the graphene. Dose response curves in seawater were evaluated with added trace levels of four heavy metals (Cd, Cu, Hg and Pb) along with detection algorithms based on machine learning and library development for each type of graphene and its modification.

15. SUBJECT TERMS

Electrochemistry test cell
Epitaxial graphene
Water analysis
Heavy metals and polyfluoroalkyl-compounds
Cyclic square wave voltammetry

16. SECURITY CLASSIFICATION OF:			**17. LIMITATION OF ABSTRACT**	**18. NUMBER OF PAGES**	**19a. NAME OF RESPONSIBLE PERSON**
					Scott Trammell
a. REPORT	**b. ABSTRACT**	**c. THIS PAGE**	U	21	**19b. TELEPHONE NUMBER** *(include area code)*
U	U	U			(202) 404-6063

Standard Form 298 (Rev. 8-98)
Prescribed by ANSI Std. Z39.18

This page intentionally left blank.

CONTENTS

FIGURES

EXECUTIVE SUMMARY

The electrochemical detection of heavy metals and polyfluoroalkyl-compounds are reported using an inexpensive in-house built potentiostat, the CStat. For heavy metal detection, two types of epitaxial graphene were used as a working electrode; multilayer graphene and hydrogen-intercalated, quasi-freestanding bilayer graphene. In addition, the graphene types were modified with an O_2 plasma etch to introduce oxygen chemical groups to the surface of the graphene. Dose response curves in seawater were evaluated with added trace levels of four heavy metals (Cd, Cu, Hg and Pb) along with detection algorithms based on machine learning and library development for each type of graphene and its modification.

For polyfluoroalkyl-compounds, the indirect electrochemical detection of perfluorooctanesulfonic acid is reported using molecularly imprinted polymers on screen printed electrodes. There was a significant signal response of the redox probe at polymer defect sites giving a large background current. The second year of the project will be exploring the use of multilayer graphene and hydrogen-intercalated, quasi-freestanding bilayer graphene as a flatter substrate for molecularly imprinted polymers, which should reduce the amount of polymer defect sites thus decreasing the background current.

This page intentionally left blank.

1. INTRODUCTION

Developing miniaturized sensors for electroanalytical measurements continues to be a dynamic field for a variety of analytical applications in field environments.[1-5] This NRL memorandum reports our FY21 NISE-funded effort to build our current programs by combining both direct electrochemical detection and identification using machine learning (ML) and library algorithms with indirect detection of electrochemically inactive compounds using molecularly imprinted polymers (MIPs). Our electrochemical strategies are highlighted in Figure 1.

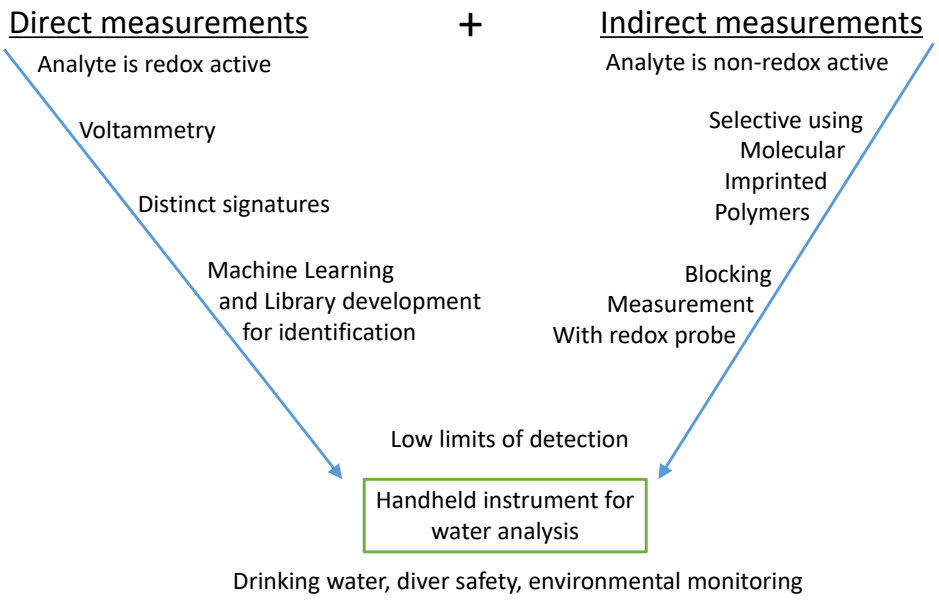

Figure 1. Electrochemical strategies for a handheld instrument for water analysis.

Our instrument, the CStat, is an inexpensive, in-house built potentiostat that was developed for the electrochemical detection of compounds in challenging environments such as explosives in sands and soils, and for heavy metals and relevant industrial contaminants in salt water for diver safety applications. In this regard, we have developed a configurable sensor that can be implemented in robotic platforms for remote monitoring in aquatic natural environments[6] and have demonstrated that multilayer epitaxial fabricated graphene is a stable working electrode for the trace analysis of chemicals in seawater.[7]

Contaminants in water of interest to the U.S. Military are heavy metals (**mercury, cadmium, selenium, arsenic**), herbicide/pesticides (**methyl parathion, paraquat**, **carbofuran**,

Manuscript approved Month 00, 2021.

methamidophos, terbufos, fenamiphos, and aldicarb) and industrial compounds (**phenol,** *fluoroacetate, and polyfluoroalkyl-compounds (PFAS)*).[8] The compounds labeled in bold are electrochemically active and therefore straightforward to identify with machine learning and library algorithms. In contrast, contaminants identified by italics give poor electrochemical signals and will need an indirect approach for trace detection using MIPs at graphene electrodes.

In this report we focused on electrochemical detection in water of the heavy metals mercury, cadmium, copper and lead, and the polyfluoroalkyl substance perfluorooctanesulfonic acid. For the heavy metals and dose response curves, machine learning algorithms were employed to evaluate the performance of the different modifications. Machine learning is widely utilized for sample classification of sensor data. We have previously shown that a number of different machine learning models can classify electrochemical signatures with high accuracy.[7, 9] In this work we use a combination of dose-response curves and machine learning to demonstrate automatic identification as well as to evaluate the performance of the different combinations of electrode modifications.

Our strategy for compounds that give a poor direct electrochemical signal focuses on the use of molecular imprinted polymers.[10-12] Recent literature success has shown the detection of PFAS using MIPs at glassy carbon electrodes; however, the response requires an advanced electrochemical technique using impedance spectroscopy to achieve the required limits of detection.[13] In addition, reduced graphene oxide has been used as a working electrode for MIPs since graphene has several promising electrochemical properties including a large electron delocalization, strong adsorption for aromatic materials, and high electronic conductivity.[14]

We have been successful using epitaxial graphene as a working electrode synthesized by sublimation of silicon from silicon carbide and its various modifications for direct electrochemical detection, [7, 15-17] and we believe that using epitaxial graphene as the working electrode for MIPs should improve the signal response. In that regard, we report on our initial work for the indirect measurement for the detection of PFAS using molecular imprinted polymers using a redox probe to measure the binding and blocking at screen printed gold electrodes with the goal to implement MIPs to epitaxial graphene materials in the second year.

2. EXPERIMENTAL

2.1 Materials

Cadmium chloride ($CdCl_2$), copper sulfate pentahydrate ($CuSO_4$), mercury chloride ($HgCl_2$) and lead chloride ($PbCl_2$), the potassium salt of heptadecafluorooctanesulfonic acid (PFOS), o-phenylenediamine (o-PD) (8 mg tablets from SigmaFast) and ferrocenemethanol (Fc-OH) were purchased from Sigma-Aldrich (St. Louis, MO). Heavy metal stock solutions were prepared at 10 mg/mL in distilled water and then diluted to 0.1 mg/mL for testing. For lead chloride, a small amount of 1M NaOH and mild heating was used to aid dissolution. Seawater samples, were collected at 20 feet below the surface at a latitude of 38.4735 and longitude of -74.89152, off Ocean City, MD. The conductivity of the seawater sample was 46 mS/cm and the pH was 7.85. The collected seawater was stored at 4°C. Stock solutions of PFOS were prepared in methanol.

2.2 Graphene synthesis, oxygen plasma modification and surface characterization

Epitaxial graphene was synthesized by sublimation of silicon from silicon carbide (SiC) substrates at high temperatures in a commercial chemical vapor deposition reactor.[7, 17-18] Substrates were first raised to growth temperature under hydrogen flow to remove polishing damage. Hydrogen-intercalated, quasi-freestanding bilayer graphene was grown on semi-insulating, on-axis 6H-SiC(0001) for 20 min at 1595°C in argon ambient, then annealed at 1050°C in hydrogen for 1 hr.[19-20] Multilayer epitaxial graphene was grown on N+, 4H-SiC(0001) with a 4° offcut towards the $[11\bar{2}0]$ direction at 1555°C for 20 min in argon ambient.

Oxygen plasma modification was performed using a Plasma Preen-II-973 microwave plasma system. Graphene samples were exposed to 100 W plasma for 15 s under ~1.5 standard cubic feet per hour oxygen flow. The surfaces of the graphene samples were characterized by atomic force microscopy (AFM), X-ray photoelectron spectroscopy (XPS) and Raman spectroscopy before and after oxygen plasma exposure. For AFM, a Bruker Dimension FastScan instrument in tapping mode was used. XPS measurements were made using a Thermo Scientific Nexsa spectrometer with a monochromatic Al-Kα source (1486.68 eV) and 400 μm spot size. High-resolution scans of the carbon 1s peak were acquired using 20 eV pass energy and 0.1 eV step size. Peak fits were performed using Avantage software. A Thermo DXRxi Raman Microscope was used to obtain 20

x 20 um^2 maps of Raman spectra in 0.3 μm x and y stage increments using a 532 nm laser at 9.6 mW and 100x objective.

2.3 Electrochemistry

A custom-built potentiostat (the CStat v3.79), used for all assays reported in this study, has been demonstrated previously for electrochemical detection of multiple compounds, including nitrogen-containing explosives, heavy metals, herbicides, pesticides, and industrial chemicals. [6-7, 9] The graphene working electrodes were mounted in a custom-made Teflon cell.[15] The funnel-shaped cell allowed the counter and reference electrodes to be suspended above the graphene. An 8 x 8 mm^2 piece of graphene was used as the working electrode along with a compact spiral platinum counter electrode (99.9% Pt, Metrohm) and an Ag/AgCl reference electrode (Metrohm). Ni/Au (20 nm/50 nm) contact pads were electron-beam evaporated (FerroTec Temescal) onto all four corners of the graphene using a foil shadow mask to facilitate electrical connection to a copper clip wired to the potentiostat.

The heavy metal determination was made in 1 mL seawater samples, which were placed into the Teflon sample cell. The reference and counter electrodes were inserted into the liquid from above. The solution was mixed to remove any air bubbles. A background cyclic square wave voltammogram was taken as the negative control. The heavy metal was added from 1 to 30 μL to give a final concentration range of 100-3000 ppb. Concentrations were measured three times and peak heights in the anodic square wave voltammetry were used to generate dose response curves. Parameters used for cyclic square wave voltammetry included two accumulation steps at two minutes each, a square wave frequency of 17.5 Hz, and a potential range from +1.0 to −1.0 V vs. Ag/AgCl. Dose response curves were generated for each heavy metal using the net peak current from the measured anodic cyclic square wave voltammograms.

2.4 Machine learning

Training and evaluation of machine learning models for classifying metals was performed as previously described with some modifications.[7, 9] The different models using Long Short-Term Memory (LSTM), Fully Convolutional Networks (FCN), and variants were implemented in Keras. Models were trained for 1000 epochs. Each library from the different materials were split into train and test sets at a ratio of 60:40. No data preprocessing was performed prior to training aside from

concatenation of cathodic and anodic scans (cathodic followed by anodic). Sample classes were defined by either metal or metal-concentration. Receiver Operation Characteristic (ROC) curves, confusion matrices, and barplots for visualizing the prediction results were generated using ggplot2 in R.[21] Micro-average area under the curve (AUC) was used as a metric for comparing model and material performance. For final evaluation of the LSTM model on a set of holdout samples, six samples were randomly selected from the total oxygen modified hydrogen-intercalated graphene dataset: Cu_2500, Hg_2500, Hg_3000, Pb_200, Pb_2500, and seawater_0, where the prefix corresponds to the metal (or seawater) and the number is the concentration of the metal in ppb.

Dose response curves were fitted using the nonlinear least squares function in the R stats package. Data was obtained by extracting the maximum anodic stripping peaks and then normalizing by subtracting background using a point selected from 0.512 V, vs Ag/AgCl (or point #880 within the vector created by the concatenated scan). Linear, sigmoidal, or hyperbolic equations were used according to which had the lowest mean standard error. Plots were produced using ggplot2 in R.[21]

2.5 Molecularly Imprinted Polymers and PFOS detection

Electropolymerization at gold screen printed electrodes (Conductive Technology) was performed with a 2:1 (v/v) mixture of 0.1 M acetate buffer (pH = 5.8) and methanol containing 10 mM o-PD and 1 mM PFOS. Cyclic voltammograms were recorded for 25 cycles in a potential window of 0−1 V vs Ag/AgCl at a scan rate of 200 mV/s. To remove the PFOS, the imprinted electrodes were soaked in 50:50 water methanol solution with slight stirring for 30 min to 1 hr. PFOS detection was performed in PBS buffer with the MIP electrodes using a redox probe ferrocenemethanol. Parameters used for square wave voltammetry was a square wave frequency of 17.5 Hz, and a potential range from 0 to 0.5 V vs. Ag/AgCl. Dose response curves were generated by measuring the absolute net peak current decrease of the ferrocenemethanol probe as a function of PFOS concentration. The results were fit to a Langmuir binding isotherm.

3. RESULTS

3.1 Graphene modification

The surface of graphene can be altered to increase its electroanalytical performance for trace detection by a variety of modifications[22] including a plasma etch to add chemical functional groups at the surface of the graphene.[17, 23] In this study, comparisons were made between multilayer epitaxial graphene and quasi-freestanding bilayer epitaxial graphene. The two types were tested for measuring heavy metals in seawater using anodic stripping cyclic square wave voltammetry with or without an oxygen plasma modification. It was hypothesized that adding oxygen functional groups to the surface of graphene would increase sensitivity by increased binding of the heavy metals via the addition of oxygen chelating groups.

The graphene samples were characterized by AFM, XPS, and Raman spectroscopy. As shown in Figure 2A and B, the multilayer graphene had a higher RMS roughness (9.5 nm) compared to hydrogen-intercalated graphene (1.8 nm). Based on maps of the FWHM of the Raman 2D peak (Figure 2C and D), the thickness of the hydrogen intercalated graphene is 2 monolayers with some areas of 3 or more monolayers (average 2D peak FWHM = 59 cm^{-1}), whereas the multilayer graphene is thicker, consisting mainly of 3 or more monolayers (average 2D peak FWHM = 71 cm^{-1}).[24] The oxygen functionally imparted to the samples by the O_2 plasma is shown by the XPS data in Figure 2E and F, in which the carbon 1s spectra shows an increase in peaks attributed to C=O and C-O after oxygen plasma exposure.

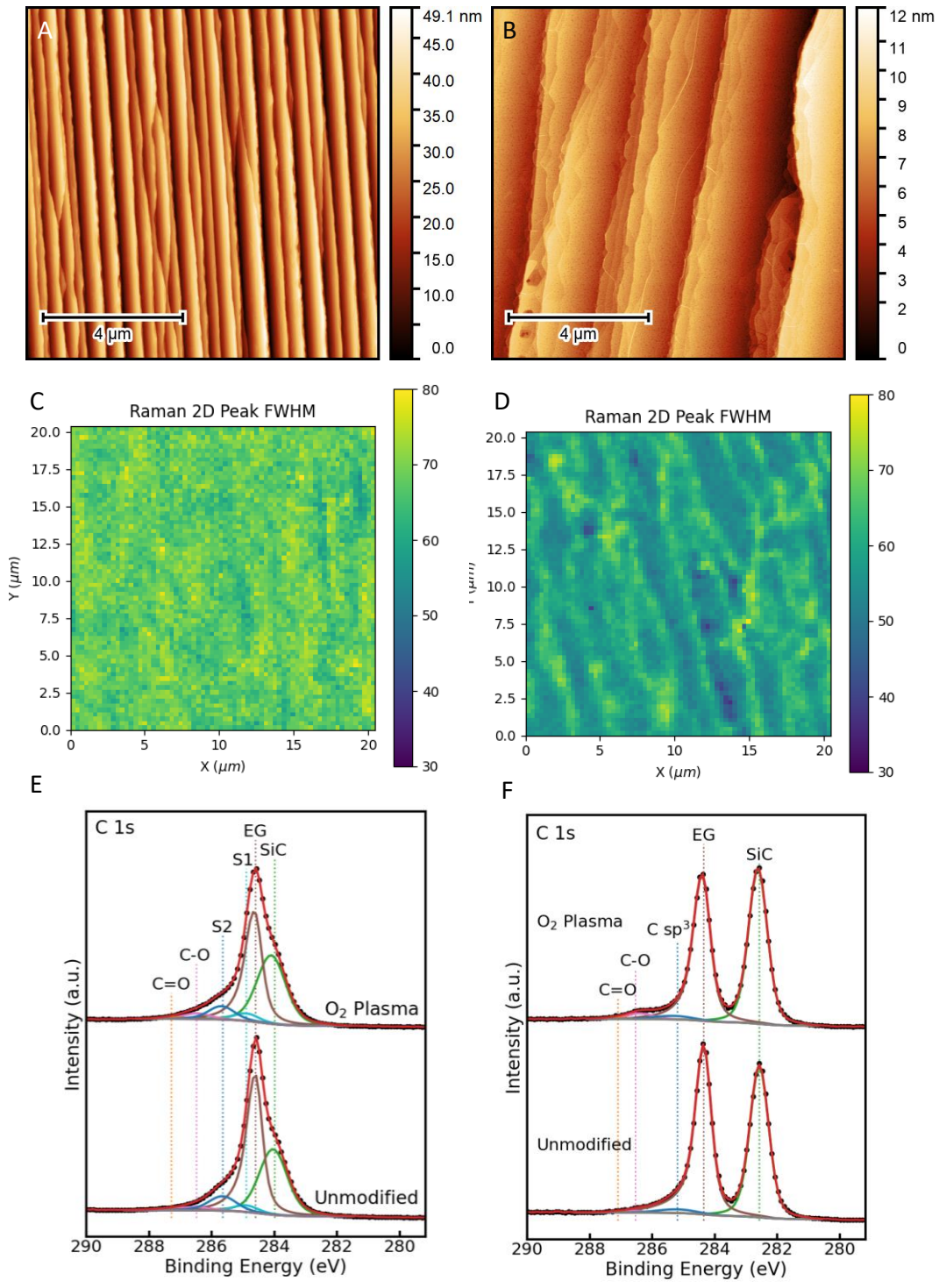

Figure 2. Surface characterization of graphene. AFM images of as-grown (A) multilayer graphene and (B) hydrogen-intercalated graphene. Maps of the full width at half maximum (FWHM) of the Raman 2D peak for unmodified (C) multilayer and (D) hydrogen-intercalated graphene. Carbon 1s XPS spectra of (E) multilayer, and (F) hydrogen-intercalated graphene before and after O_2 plasma modification.

3.2 Heavy metal detection at modified graphene with machine learning

Graphene electrodes were studied further using seawater samples with additions of four heavy metals, Cd, Cu, Hg and Pb. As shown in Figure 3A, for the various heavy metal cations, the cathodic peaks are concomitant with oxygen reduction, and the anodic stripping peaks have their respective peak potentials.[7] Using these distinctive peaks for each metal from the cyclic square wave voltammograms, the dose response in current between 100–3000 ppb for each analyte was plotted in Figure 3E. The dose response displayed was dependent on the analyte and type of graphene used. For both $CuSO_4$ and $CdCl_2$, dose response was consistent for each material used, where the best non-linear fits were hyperbolic (Equation (1)) and sigmoidal (Equation (2)) curves, respectively. The dose responses for $HgCl_2$ and $PbCl_2$ were more complex as both metals displayed different responses for either multilayer or hydrogen-intercalated graphene. $HgCl_2$ showed a linear response on multilayer graphene, but sigmoidal on hydrogen-intercalated graphene. Similarly, $PbCl_2$ was observed to have a sigmoidal response on multilayer graphene while appearing hyperbolic on hydrogen-intercalated graphene (Figure 3E). Whether the graphene was O_2-modified did not appear to influence the response.

$$f = \frac{ax}{1+bx} \tag{1}$$

$$f = \frac{a}{1+ e^{\frac{-(x-x_0)}{b}}} \tag{2}$$

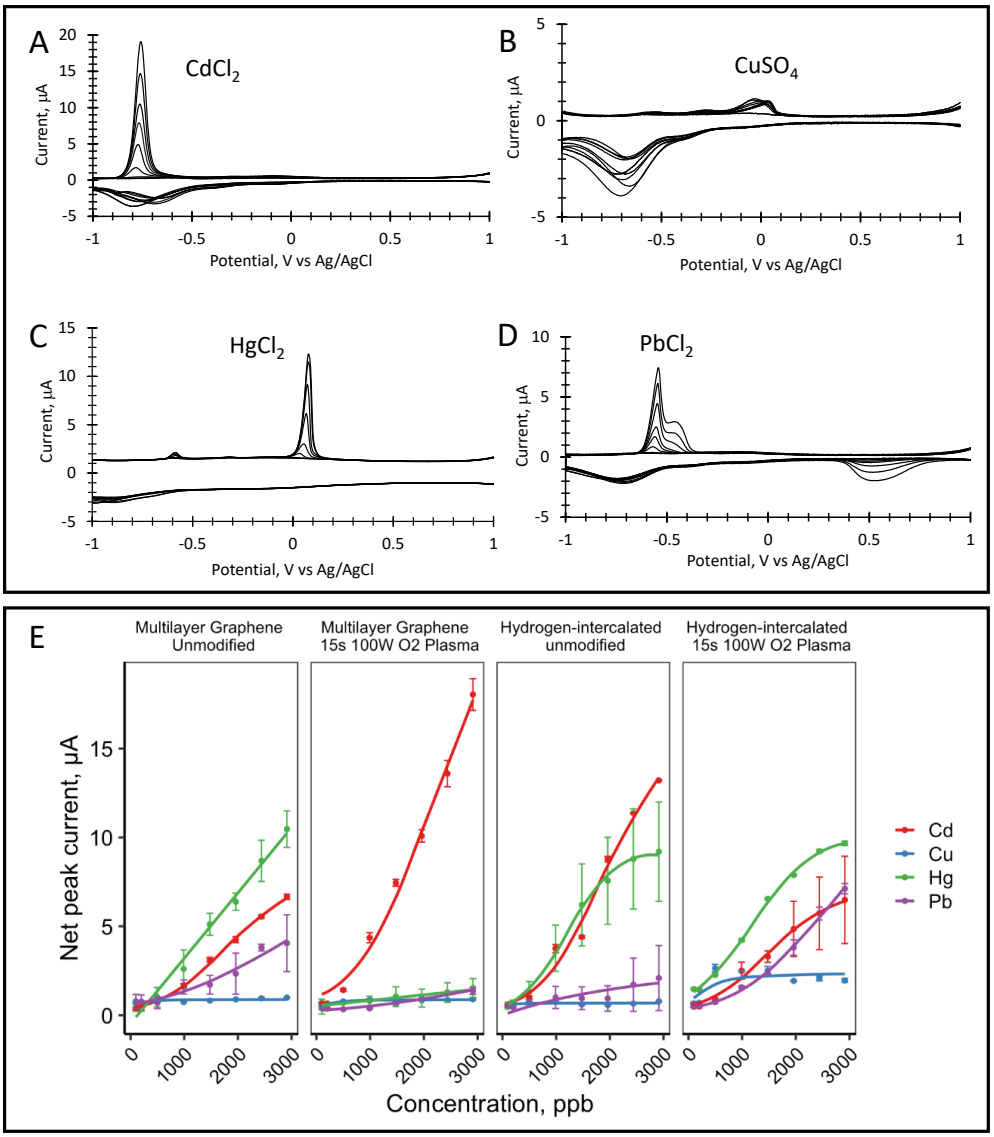

Figure 3. Examples of cyclic square wave voltammograms and the dose response of heavy metals in seawater between 0 to 3 ppm. **A**. $CdCl_2$ at oxygen modified multilayer graphene. **B**. $CuSO_4$ at unmodified multilayer graphene. **C**. $HgCl_2$ at unmodified hydrogen-intercalated graphene. **D**. $PdCl_2$ at oxygen modified hydrogen-intercalated graphene. **E** Dose response curves for each type of graphene and modification.

The previous strategy for data processing was used prior to training for the machine learning analysis, which included the concatenation of cathodic and anodic scans for each sample, but otherwise the experimental data was not modified.[9] The confusion matrix for the complete set of data as well as the ROC curves and area under the ROC curves are shown in Figure 4. Four ML models (LSTM, FCN, LSTM-FCN, and ALSTM-FCN) were each trained on the four different graphene types. Each of the metals had a high degree of correct identification, with the most

consistent misclassification being seawater predicted as metal or vice versa. The results differ widely according to model and graphene type. The difference in model performance as the result of material is most clearly seen in the significantly higher correct IDs in oxygen modified hydrogen-intercalated graphene (Figure 4D) relative to unmodified multilayer graphene (Figure 4A). The differences in performance between the four different models was less clear. Using the area under the curve values of the ROC curves (Figure 4E), the average AUC for the four models for unmodified multilayer graphene was 0.972, while the average for oxygen modified hydrogen-intercalated graphene was significantly higher at 0.998. Unmodified hydrogen-intercalated graphene had an average area under the ROC curve of 0.986 and oxygen modified multilayer graphene was 0.995.

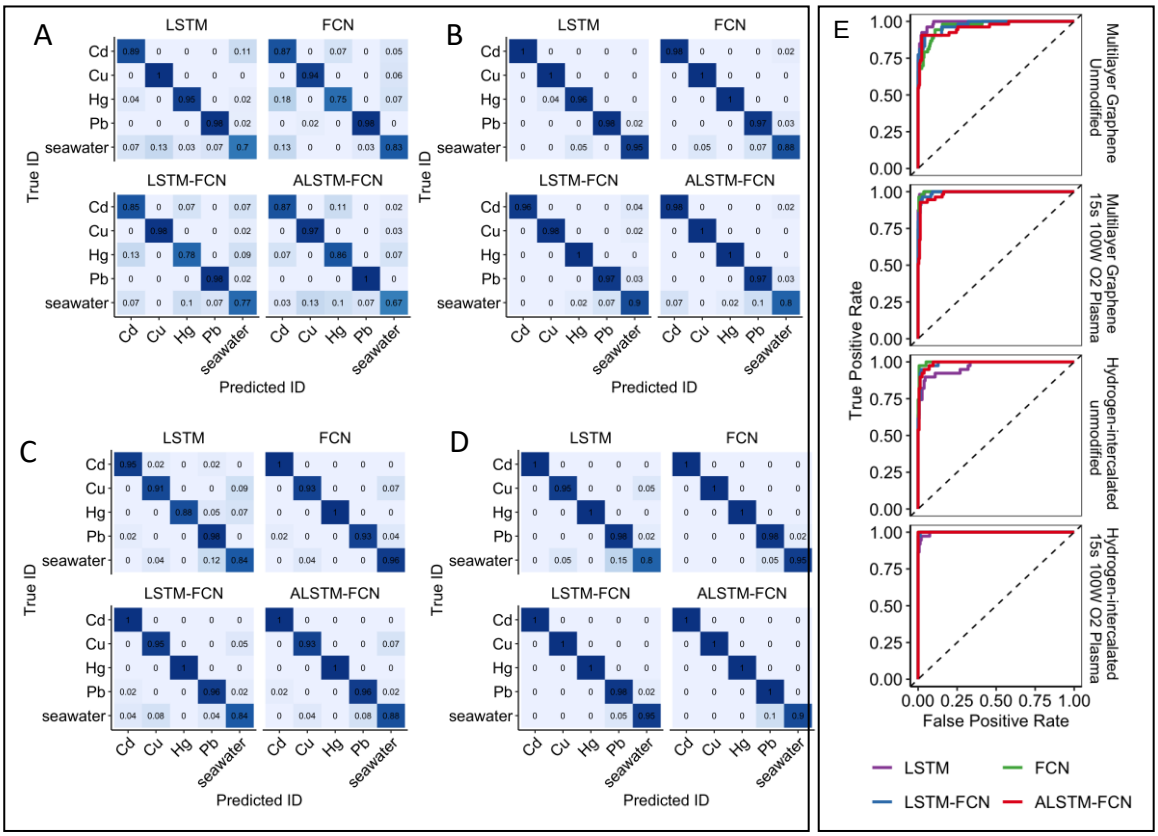

Figure 4. Confusion matrixes comparing the different machine learning models for the library of cyclic square wave voltammograms of seawater spiked with heavy metals at different types and modifications of graphene. **A**. Multilayer graphene. **B**. Oxygen modified multilayer graphene. **C**. Hydrogen-intercalated graphene. and **D**. Oxygen modified hydrogen-intercalated graphene. **E**. Receiver Operating Characteristic (ROC) curves for same data comparing the different machine learning models with the different types and modifications of graphene.

Using the best-performing model-material pair, ALSTM-FCN and oxygen modified hydrogen-intercalated graphene was evaluated for its ability to classify both metal and concentration simultaneously (Figure 5A). In an experiment with repeated shuffle and split cross-validation, the observed performance was promising. With few exceptions, including the misclassifications of 200 ppb Pb and Cd as seawater or vice versa, each of the classifications was either correct or confined to the metal class. In particular, the model had difficulty distinguishing between higher concentrations (1000, 1500, and 2000 ppb) of Cd, but none were misassigned as a different metal.

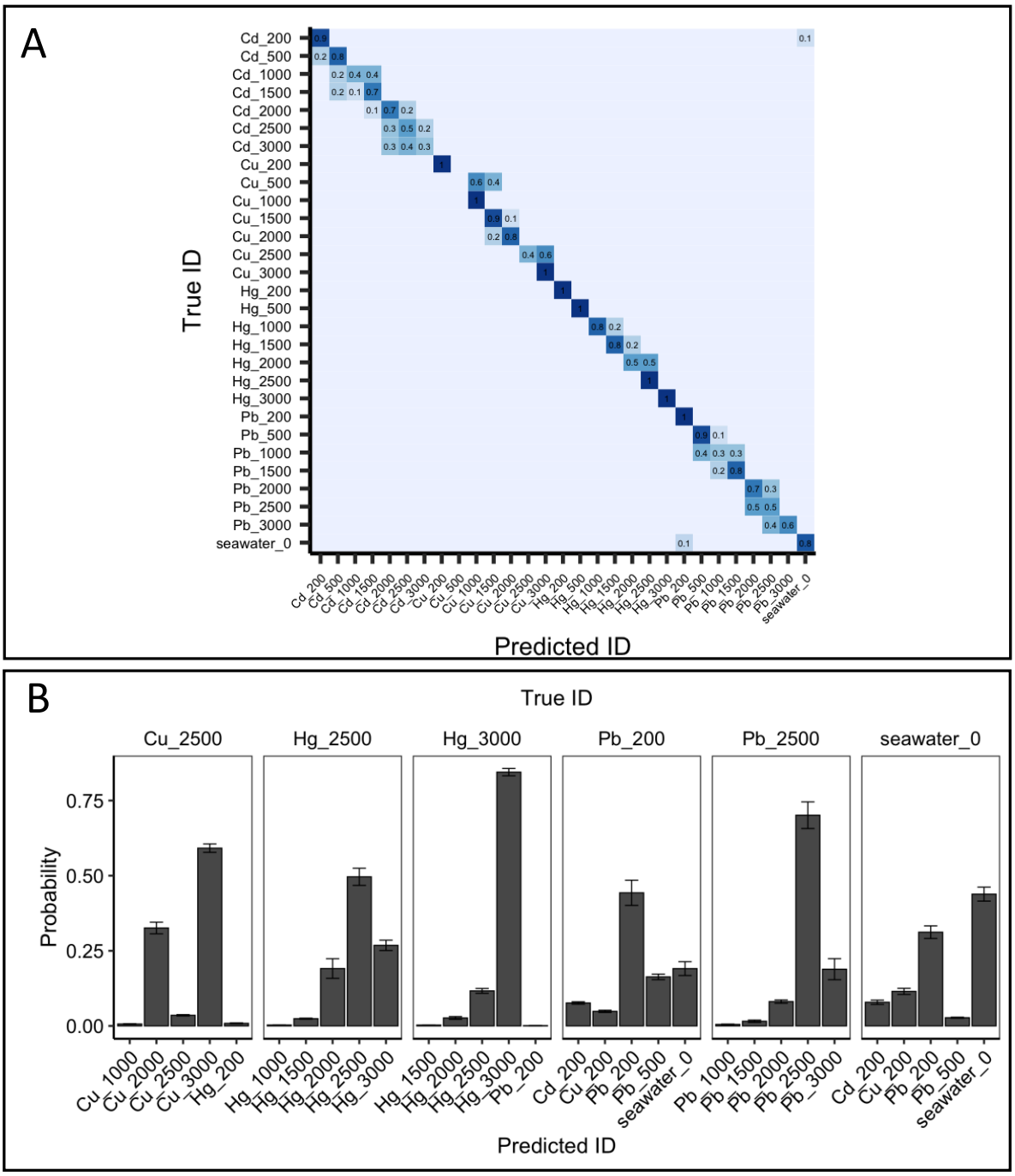

Figure 5. ML model prediction of concentration using oxygen modified hydrogen-intercalated graphene data. **A.** Confusion matrix results using ALSTM-FCN to predict both metal and concentration. The prefix corresponds to the metal (or seawater) and the suffix is the concentration in ppb. Probabilities of 0 are removed for clarity. **B.** Evaluation of holdout dataset. Both identity and concentration of six samples selected at random (true IDs listed at the top) were evaluated for prediction performance. The top five predicted IDs according to probability for each sample are shown.

Next, the best-performing model-material pair was evaluated on a small set (n = 6) of holdout samples as further confirmation of performance, and to further evaluate the range of probabilities assigned to different compounds (Figure 5B). Here, Cu_2500, Hg_2500, Hg_3000, Pb_200, Pb_2500, and seawater_0 were randomly selected for evaluation and the top five predicted IDs according to probability for each were plotted. Consistent with the confusion matrix, the only misclassification (here, the highest probability assigned) was Cu_2500 as Cu_3000. The only additional issues resulted from low concentrations (200 ppb) and seawater, due to the lower signals from the metals, and these samples are still likely to be classified correctly.

3.3 Molecularly imprinted polymers for PFOS detection

The initial work focuses on the development of an assay for perfluorooctanesulfonate (PFOS) focused on molecular imprinted polymers. The MIPs process is illustrated in Figure 6. O-phenylenediamine was incubated with the target of interest (i.e. PFOS) and then electro-polymerized onto the surface of the electrode, followed by embedded target removal with solvent.

The result was an imprinted electrode that is sensitive to adsorption from the target compound. Similar to enzymes, target selectivity is based on its shape. Because the polymer is an insulator, the only useable portions of the electrode are those that were imprinted. In the absence of target, oxidation and reduction by small molecules can take place within the imprinted regions. In the presence of a target, some or all of the imprinted regions will be blocked. The amount of blocked region is based on the target adsorption isotherm; this can be quantitatively measured by monitoring the activity of an auxiliary small molecule reaction such as the reduction of ferrocenemethanol.

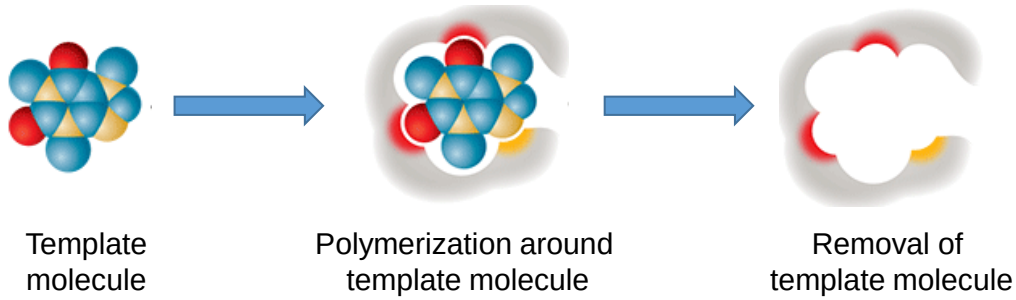

Figure 6. Polymerization of molecularly imprinted polymers

As shown in Figure 7, polymerization of molecularly imprinted o-PD for PFOS was successful at screen printed gold electrodes. As the PFOS concentration increases, more of the binding sites generated by the polymerization of molecularly imprinted o-PD were bound by PFOS, which simultaneously showed a decrease in the electrochemical signal for the redox probe as the electrode become more blocked. However, only a portion of the redox probe was blocked which suggests there are defect sites at the polymer/electrode interface which are not imprinted. Screen printed electrodes tend to have higher roughness compared to graphene which is very flat. Our hypothesis is the flatter graphene should generate a more defect free polymer film.

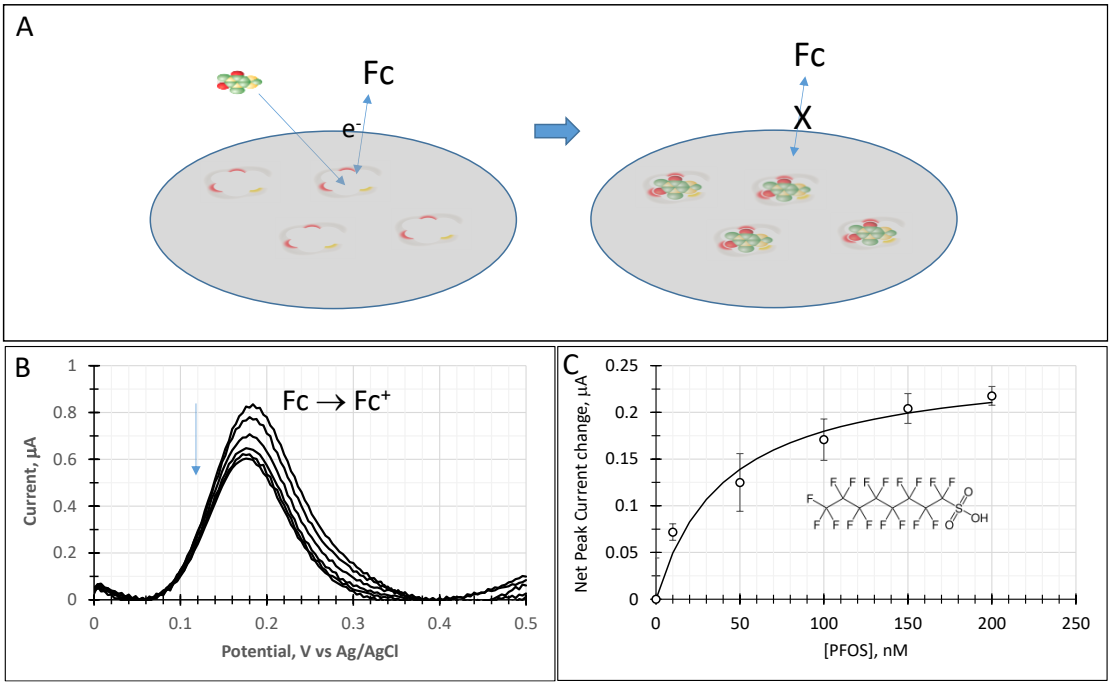

Figure 7. Indirect electrochemical detection of PFOS using ferrocenemethanol at a molecularly imprinted modified screen printed gold electrode. **A**. A schematic showing the blocking of the redox probe as PFOS binds to the imprinted sites at the electrode. **B**. The square wave voltammetry of the ferrocenemethanol redox probe as the concentration of the PFOS increases. C. A plot of the absolute net change in current as a function of PFOS concentration with the data fit to a Langmuir binding isotherm.

4. CONCLUSION

Using an electrochemical strategy to include both direct and indirect electrochemical detection, we have shown that a small custom-built potentiostat can be used for the detection of heavy metals and polyfluoroalkyl-compounds. We envision a final device will have excellent SWaP

characteristics; it will run on rechargeable NiMH batteries; and it can be interfaced with a laptop computer or an Android cell phone through a wireless Bluetooth connection. The focus of the second year will be to reduce the limits of detection with graphene modification, tethered redox probes and algorithm development for facile field measurements.

5. REFERENCES

1. Denuault, G., Electrochemical techniques and sensors for ocean research. *Ocean Sci.* **2009,** *5*, 697–710.
2. Mills, G.; Fones, G., A review of in situ methods and sensors for monitoring the marine environment. *Sensor Review* **2012,** *32* (1), 17-28.
3. Taillefert, M.; III, G. W. L.; Nuzzio, D. B., The Application of Electrochemical Tools for In Situ Measurements in Aquatic Systems. *Electroanalysis* **2000,** *12* (6).
4. Johnson, K. S.; Needoba, J. A.; Riser, S. C.; Showers, W. J., Chemical Sensor Networks for the Aquatic Environment. *Chem Rev* **2007,** *107* (2), 625.
5. Justino, C. I. L.; Freitas, A. C.; Duarte, A. C.; Santos, T. A. P. R., Sensors and biosensors for monitoring marine contaminants. *Trends in Environmental Analytical Chemistry* **2015,** *6-7*, 21-30.
6. Erickson, J. S.; Shriver-Lake, L. C.; Zabetakis, D.; Stenger, D. A.; Trammell, S. A., A Simple and Inexpensive Electrochemical Assay for the Identification of Nitrogen Containing Explosives in the Field. *Sensors (Basel)* **2017,** *17* (8), 1769.
7. Shriver-Lake, L. C.; Myers-Ward, R. L.; Dean, S. N.; Erickson, J. S.; Stenger, D. A.; Trammell, S. A., Multilayer Epitaxial Graphene on Silicon Carbide: A Stable Working Electrode for Seawater Samples Spiked with Environmental Contaminants. *Sensors* **2020,** *20*, 4006.
8. Water Sensors Community of Practice DOD Workshop. U.S. ARMY COMBAT CAPABILITIES DEVELOPMENT COMMAND SOLDIER CENTER, 2020.
9. Dean, S. N.; Shriver-Lake, L. C.; Stenger, D. A.; Erickson, J. S.; Golden, J. P.; Trammell, S. A., Machine Learning Techniques for Chemical Identification Using Cyclic Square Wave Voltammetry. *Sensors (Basel)* **2019,** *19* (10), 2392.
10. Zarejousheghani, M.; Rahimi, P.; Borsdorf, H.; Zimmermann, S.; Joseph, Y., Molecularly Imprinted Polymer-Based Sensors for Priority Pollutants. *Sensors (Basel)* **2021,** *21* (7).
11. BelBruno, J. J., Molecularly Imprinted Polymers. *Chem Rev* **2019,** *119* (1), 94-119.
12. Rebelo, P.; Costa-Rama, E.; Seguro, I.; Pacheco, J. G.; Nouws, H. P. A.; Cordeiro, M.; Delerue-Matos, C., Molecularly imprinted polymer-based electrochemical sensors for environmental analysis. *Biosensors & bioelectronics* **2021,** *172*, 112719.
13. Clark, R. B.; Dick, J. E., Electrochemical Sensing of Perfluorooctanesulfonate (PFOS) Using Ambient Oxygen in River Water. *ACS Sens* **2020,** *5* (11), 3591-3598.
14. Luo, J.; Cong, J.; Liu, J.; Gao, Y.; Liu, X., A facile approach for synthesizing molecularly imprinted graphene for ultrasensitive and selective electrochemical detecting 4-nitrophenol. *Anal Chim Acta* **2015,** *864*, 74-84.
15. Zabetakis, D.; Shriver-Lake, L. C.; Erickson, J. S.; Trammell, S. A.; Hajzus, J. R.; Pennachio, D. J.; Myers-Ward, R. L. *Demonstration of a Teflon Electrochemical Test Cell for Epitaxial Graphene*; NRL/6930/MR—2021/1; 2021.

16. Trammell, S. A.; Myers-Ward, R. L.; Hangarter, S. C.; Gaskill, D. K.; Zabetakis, D.; Stenger, D. A.; Walton, S. G. Plasma modified epitaxial fabricated graphene on SiC for electrochemical trace detection of explosives. US 10,928,351 B2, Feb. 23, 2021.
17. Trammell, S. A.; Hernandez, S. C.; Myers-Ward, R. L.; Zabetakis, D.; Stenger, D. A.; Gaskill, D. K.; Walton, S. G., Plasma-Modified, Epitaxial Fabricated Graphene on SiC for the Electrochemical Detection of TNT. *Sensors (Basel)* **2016,** *16* (8), 1281.
18. Nyakiti, L. O.; Wheeler, V. D.; Garces, N. Y.; Myers-Ward, R. L.; Eddy, C. R.; Gaskill, D. K., Enabling graphene-based technologies: Toward wafer-scale production of epitaxial graphene. *Mrs Bull* **2012,** *37* (12), 1149-1157.
19. Daniels, K. M.; Jadidi, M. M.; Sushkov, A. B.; Nath, A.; Boyd, A. K.; Sridhara, K.; Drew, H. D.; Murphy, T. E.; Myers-Ward, R. L.; Gaskill, D. K., Narrow plasmon resonances enabled by quasi-freestanding bilayer epitaxial graphene. *2d Materials* **2017,** *4* (2), 025034.
20. Emery, J. D.; Wheeler, V. H.; Johns, J. E.; McBriarty, M. E.; Detlefs, B.; Hersam, M. C.; Gaskill, D. K.; Bedzyk, M. J., Structural consequences of hydrogen intercalation of epitaxial graphene on SiC(0001). *Applied Physics Letters* **2014,** *105* (16), 161602.
21. Team, R. C. *R: A language and environment for statistical computing*, R Foundation for Statistical Computing: Vienna, Austria, 2019.
22. Chang, J.; Zhou, G.; Christensen, E. R.; Heideman, R.; Chen, J., Graphene-based sensors for detection of heavy metals in water: a review. *Anal Bioanal Chem* **2014,** *406* (16), 3957-75.
23. Trammell, S. A.; Myers-Ward, R. L.; Hangarter, S. C.; Gaskill, D. K.; Zabetakis, D.; Stenger, D. A.; Walton, S. G. Plasma modified epitaxial fabricated graphene on SiC for electrochemical trace detection of explosvies. US 10,928,351 B2, Feb. 23, 2021.
24. Lee, D. S.; Riedl, C.; Krauss, B.; von Klitzing, K.; Starke, U.; Smet, J. H., Raman spectra of epitaxial graphene on SiC and of epitaxial graphene transferred to SiO2. *Nano Lett* **2008,** *8* (12), 4320-5.